MSW MANAGEMENT -Multidisciplinary, Scientific Work and Management Journal
ISSN: 1053-7899
Vol. 36 Issue 1s, 2026, Pages: 4135-4140

Magnetic Control of Nanofluid Transport in Porous Media under Variable Viscosity and Thermal Conductivity

Dr. Bhagwan Singh[1], Ravi Kumar[2], Dr. Prabal Pratap Singh[3*]
[1]*Assistant Professor, Department of Mathematics, V. A. Government Degree College, Atrauli, Aliagrh (India)*
[2]*Research Scholar, Department of Mathematics, V. A. Government Degree College, Atrauli, Aliagrh (India)*
[3*]*Professor, Department of Mathematics, J.S. University, Shikohabad, Uttar Pradesh, India*
Email id of corresponding Author: drppsingh0508@gmail.com

Abstract
The objective of this research is to determine how a magnetic field influences nanofluid transport within a porous medium due to both the variations of fluid viscosity and thermal conductivity. A two dimensional steady state flow model was developed to examine the magnetohydrodynamic effects, Darcy resistance and the temperature dependence of the fluids' properties. The governing nonlinear equations for momentum (velocity), energy (temperature) and concentration (nanoparticles) were reduced from partial differential to ordinary differential equations using similar variables. The Homotopy Perturbation Method was then used to find an analytical solution of these coupled ODEs which would provide closed form solutions for the velocity, temperature and concentration fields. A detailed examination was performed on the effect of several significant physical parameters including the magnetic parameter, the Prandtl number, the Eckert number, the thermal conductivity variation, thermophoresis and the Lewis number. It was demonstrated that the magnetic field has a large impact on reducing the motion of the fluid; while varying the thermal conductivity and viscous dissipation have a positive impact on increasing thermal transport. Thermophoresis and mass diffusivity also greatly affect the distribution of nanoparticles. The analytical results of the present model show good agreement with the previous models and therefore confirm that the current model is accurate and physically relevant.

Keywords: Magnetohydrodynamics, nanofluid flow, porous medium, variable viscosity, variable thermal conductivity, homotopy perturbation method, thermophoresis, heat and mass transfer

1. INTRODUCTION:

Magnetohydrodynamic (MHD) nanofluid flow through porous media has recently attracted significant interest from researchers as well as engineers, because of its broad range of applications such as; geothermal energy production, thermal insulation systems, biomedical processes and new cooling techniques. An MHD system offers an efficient method to control flow and heat transfer characteristics of electrically conducting nanofluids and is therefore widely used in many practical situations. However, the viscosity and thermal conductivity of fluids are highly dependent on the temperature, and if these effects are neglected, the accuracy of prediction will be poor. Thermophoresis and Brownian motion-induced nanoparticle migration also have important influences on the transport phenomenon of mass. To investigate these effects, this study aims at developing an analytical solution based on a comprehensive model that includes both temperature-dependent viscosity and thermal conductivity of the nanofluid, MHD effects and porous resistance, and coupling between heat and mass transfers. The Homotopy Perturbation Method (HPM) is applied to obtain explicit analytical solutions of the model, which allows us to conduct a parametric analysis of the governing physical mechanisms in detail. The developed model provides a complementary and extensional approach compared to previous studies, since it accounts for all the above-mentioned effects simultaneously, and therefore contributes to provide a better understanding of the controlled nanofluid transport processes.

Shemaiah and Annand (2012) studied transient magnetohydrodynamics free convection near a vertical porous plate including suction/injection effects as well as a chemical reaction mechanism. Their study demonstrated how wall mass transfer could be manipulated to influence boundary layer thickness, buoyancy-driven flow, and the species/thermal field within the boundary layer due to magnetic damping. The study further showed that the degree of chemical reaction has a significant effect on the concentration gradient and thus the coupled momentum-mass transport characteristics; this is particularly relevant for applications involving reactive nanofluids or nanoparticle laden flows through porous structures. **Raju et al. (2016)** studied an unsteady magneto-nanofluid configuration produced by a rotating cone whose viscosity varies with temperature. Their work was framed toward biomedical/surgical implant relevance. They illustrated that the temperature dependence of viscosity substantially alters the local near-wall velocity gradients and enhances the relative importance of rotation induced forcing versus magnetic braking. Additionally, they demonstrated that magnetic damping can be employed to mitigate excessive shear and modulate thermal transport; however, the temperature dependent viscosity significantly increases the nonlinear response to time dependent forcing. **Umavathi et al. (2016)** studied free convection in a vertical channel where both viscosity and thermal conductivity varied with temperature. They illustrated that by permitting transport properties to vary, one produces asymmetric and highly coupled momentum-energy behaviors compared to constant property models. Specifically, the variable viscosity affects the effective resistance to motion throughout the channel whereas the variable thermal conductivity permits greater redistribution of heat in warmer regions thereby affecting both wall heat transfer and the core temperature level. Their work serves as a base line for later nanofluid studies illustrating how variability in transport properties alone can mimic or enhance some of the effects typically associated with nanoparticles or magnetic forcing.

The next study used the same framework as above **(Umavathi et al., 2016)**, however this study was specifically about a first order chemical reaction in a mixed convection problem. The authors were able to demonstrate that there are parameter values where either shear driven mass transfer occurs or buoyancy driven mass transfer occurs depending upon whether shear driven or buoyancy driven conditions occur. They also demonstrated that variations in fluid properties will shift the transition between these two types of mass transfer. In addition to the variations in fluid properties due to temperature, the chemical reaction added another sink/source term for the concentration of species, which was used to provide feedback to both buoyancy (if solutal effects were included) and to affect the mass transfer rate to the walls. This study is particularly relevant to porous media models of nanofluids where the three mechanisms of reaction, temperature dependent properties and convection modes often interact simultaneously. The final study examined the use of CuO-water nanofluid for enhancing heat transfer in an automotive radiator **(Sabeel & Dil, 2017)**. While the primary focus of this study was to document the improvements in heat transfer rates achieved when nanoparticles were added to water, they also provided some discussion of the trade-offs associated with increased viscosity of the nanofluid that results from the addition of particles. Increased viscosity will increase the pumping power required to circulate the fluid, and thus will negatively impact the energy efficiency of the system. As such, the focus of this study was on the practical application of using nanofluids to enhance heat transfer rates, and as such provides additional support for later studies that include evaluation of the pressure drop/energy cost associated with using a specific mechanism to improve heat transfer rates. **Reddy (2018)** developed a model of the bio-magnetic pulsatile transport of a Ti-alloy-Au/blood couple stress hybrid nanofluid in a rotating channel. The model shows how the couple stresses in the blood interact with the pulsatility and rotation to create the velocity profiles and wall shear stresses that are necessary to calculate the transport rates. The model also includes the effects of a magnetic field on the flow resistance and stability of the pulsatile pattern. Finally, the use of a hybrid particle in the Ti alloy-augmented Au blood nanofluid to produce a higher thermal conductivity than would occur if only one type of particle was present. However, the use of hybrid particles also increases the complexities of the rheological behavior of the fluid. This line of research is of interest for magnetic control concepts because it demonstrates how magnetic forcing can be used to control the flow resistance and stabilize the pulsatile flow patterns, as well as how these flow patterns are influenced by physiological style unsteadiness and rotational influences.

Sabeel and Kaneez (2020) studied the application of hybrid nanofluids, which are Cosserat (micropolar/Cosserat-type), in order to enhance the process of heat transfer through the use of a continuous Galerkin-Petrov numerical strategy. The studies by Sabeel and Kaneez show how the addition of micro-rotation and couple stresses create new ways in which momentum can diffuse in a fluid, and this diffusion may either increase or decrease the rate of convective transport depending on the specific values of the parameters chosen. In comparison to traditional hybrid nanoparticles, the Cosserat model causes the formation of the boundary layer to differ from the conventional model and the sensitivity of wall heat transfer to rheological parameters will differ due to the Cosserat model. This study suggests that if the non-classical behavior of the fluid is as significant as the amount of nanoparticle loading in the determination of heat transfer rates, then the inclusion of additional mechanisms such as advanced porous media and MHD in future research is supported. Singh et al. (2021) examined the heat and mass transfer characteristics of a titanium alloy-water nanofluid flowing over a vertical plate under the influence of Hall current and a pre-imposed magnetic field. The study by Singh et al., demonstrated that Hall currents can produce a large degree of variation in the effective Lorentz force direction and magnitude that can lead to cross-flow effects and altered momentum and thermal boundary layers. Furthermore, they showed that when Hall currents are present, magnetic braking effects are not solely dependent upon the strength of the magnetic field, but rather are influenced by the electromagnetic coupling effects of the Hall and potential ion-slip effects. Therefore, this is a critical observation for porous-channel and biomedical MHD applications, since the predicted heat transfer and shear behavior can be altered by electromagnetic micro-scale interactions. Jha and Malgwi (2022) studied the free convection of a Hall current-ion slip magnetohydrodynamic (MHD) flow within a vertical microporous channel. The studies of Jha and Malgwi demonstrated that both the flow structure and the combined effects of buoyancy forces, porous resistance, and electromagnetic coupling are determined by all three of these factors, and that the Hall/ion-slip terms can either reduce the amount of

MSW MANAGEMENT -Multidisciplinary, Scientific Work and Management Journal
ISSN: 1053-7899
Vol. 36 Issue 1s, 2026, Pages: 4135-4140

magnetic damping or redistribute the damping throughout the system. Additionally, they demonstrated that in microporous channels, the permeability of the porous medium can dictate the nature of the heat transfer, i.e. whether or not the heat transfer is boundary-layer dominated or is influenced by the core region. These findings represent a key step toward developing realistic porous-media models of nanofluids, particularly when magnetic fields are employed as active control inputs and electromagnetic corrections cannot be neglected.

Waqas et al. (2023) modeled blood circulation involving a hybrid nanofluid within an arterial stenosis using computational analysis to investigate heat exchange. Computational results demonstrated that geometric constriction magnified spatial gradients in velocity, increased shear stress at the throat of the stenosis, and altered the temperature distribution due to enhanced convective transport. Results indicated that the addition of hybrid nanoparticles would improve thermal transport capabilities; however, the study suggested that there is a need to develop risk management strategies related to shear in biomedical applications. This study is relevant to magnetic-control subjects because stenotic geometries are sensitive to external influences (magnetic or otherwise) and variation in properties can greatly affect local hot spots and wall stresses. Nadhira et al. (2024) investigated Maxwell hybrid nanofluid behavior in a region of a stagnation point on a stretching/shrinking inclined plate subjected to radiation effects and varying shapes of the nanoparticles. Results showed that viscoelasticity (Maxwell time dependent effects) changed the response of the fluid to stretching/shrinking of the surface and modified the thicknesses of both momentum and thermal layers. At higher thermal conditions, radiation became a major source of energy transport, and selection of the shape of the nanoparticles significantly affected heat transfer by modifying effective thermal conductivity and interfacial transport behavior. These results support porous-MHD extensions by demonstrating that constitutive rheological properties and morphology of nanoparticles may be able to simultaneously control heat transfer, often to the same extent as magnetic parameters.

Awang et al. (2024) studied the effects of shape and orientation on the hybrid magnetohydrodynamic mixed convection of a Jeffrey nanofluid over a vertically stretching plate in which they emphasized the role of nanoparticle shape. Their results show that the momentum diffusion process can either be delayed or accelerated by relaxation/retardation effects of the Jeffrey fluid depending on parameter balance. The alignment of the magnetic field provides a damping mechanism for control of the flow while mixed convection introduces competition between buoyancy assistance and magnetic suppression. The work clearly shows that the shape of nanoparticles is not an insignificant detail but can significantly alter wall heat transfer and skin frction, thus "magnetic control" strategies should be optimized together with morphology of the nanofluid and non-Newtonian parameters. Bhuvaneshwari et al. (2024) studied the effects of variable viscosity and variable thermal conductivity on mixed convection of a Casson nanofluid in a channel under Chemical reaction. Their results highlight that the yield stress behavior of Casson change near-wall shear distribution and can thicken the momentum layer, while variable viscosity can either increase or decrease resistance to flow depending on temperature field. Variable thermal conductivity enhances heat diffusion in warmer regions of the flow, thereby modifying wall heat transfer rates and potentially reduce thermal gradients near walls. The Chemical reaction adds coupling through species transport, thus modifying levels of species and indirectly modifying the strength of convection. This study has closest connection with your direction of thesis because it combines physics of non-Newtonian nanofluid, transport of species and effects of variable properties in a confined channel configuration. **Nazeer*et al.* (2025)** examined Poiseuille-type transport of a Jeffrey fluid in porous media with variable transport properties under magnetic and radiative influences. Their analysis demonstrates that porous drag works together with Lorentz forces to reduce flow rates, but variable viscosity and conductivity change how strongly the magnetic field influences the velocity and temperature fields across the porous domain. Radiation introduces an additional pathway for energy transport that can either enhance or diminish the net heat transfer depending on whether it effectively acts as a heat source term within the energy balance. The main value of this study is showing how multiple control mechanisms porous permeability, magnetic forcing, radiation, and temperature-dependent propertiesmust be treated simultaneously to predict heat transfer and pressure-drop behavior reliably.**Tarapuram*et al.* (2026)** analyzed Casson hybrid nanofluid flow in a porous channel focusing on variable viscosity effects in the context of thermal mechanics. Their results emphasize that property variation substantially changes the effective momentum diffusion and modifies wall shear sensitivity to magnetic/porous resistance when such effects are included in comparable frameworks. Hybrid nanoparticle combinations improve thermal transport capacity, but variable viscosity can offset or amplify these gains depending on how viscosity responds to temperature. The study supports the broader theme of magnetic control in porous channels by reinforcing that any magnetic regulation strategy must be designed with temperature-dependent rheology in mind; otherwise, predicted improvements in heat transfer may not materialize or could come with higher frictional penalties.

2. MATHEMATICAL MODELING:

2.1 Physical Setup: Consider:

(i) 2D flow in a saturated porous medium
(ii) External magnetic field $\mathbf{B_0}$ normal to the flow
(iii) Darcy–Brinkman–Forchheimer model (optional)
(iv) Nanoparticle concentration effects
(v) Temperature-dependent viscosity μ(T) and thermal conductivity k(T)

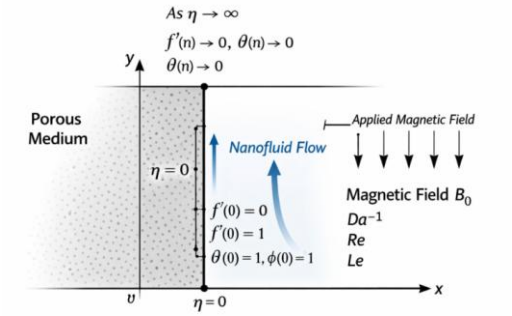

Fig. 1: Geometry & Boundary Conditions

2.2 Governing Equations:

Continuity: $\nabla . \vec{u} = 0$ (1

Momentum (MHD Brinkman model):

$\mu(T)\nabla^2\vec{u} - \frac{\mu(T)}{K}\vec{u} - \sigma B_0^2\vec{u} - \rho(\vec{u}.\nabla)\vec{u} + \nabla p = 0$ (2

Variable viscosity

Following temperature-dependent models like in Afifi et al. (2025)

$\mu(T) = \mu_\infty e^{-a(T-T_\infty)}$

(3

Energy equation with variable thermal conductivity

$\rho c_p(\vec{u}.\nabla T) = \nabla[\mathrm{k(T)}\nabla\mathrm{T}] + \mathrm{Q(T)}$

(4

$$\mathrm{k(T)} = \mathrm{k}_\infty[1 + \beta(T - T_\infty)]$$

Nanoparticle concentration

$\vec{u}.\nabla C = D_B\nabla^2 C + \frac{D_T}{T_\infty}\nabla^2 T$

(5

Non-dimensionalization

Define: $\eta = \frac{y}{L}, \theta = \frac{T-T_\infty}{T_w-T_\infty}, \phi = \frac{C-C_\infty}{C_w-C_\infty}$ (6

Resulting in dimensionless ODEs:

Momentum: $f''' + Reff'' - (M + Da^{-1})f' = 0$

(7

MSW MANAGEMENT -Multidisciplinary, Scientific Work and Management Journal
ISSN: 1053-7899
Vol. 36 Issue 1s, 2026, Pages: 4135-4140

Energy: $(1+\epsilon\theta)\theta'' + \Pr f\theta' + Ecf''^2$
Concentration: $\phi'' + Lef\phi' + Nt\theta'' = 0$

(8

3.ANALYTIC SOLUTION USING HOMOTOPY PERTURBATION METHOD (HPM):
(i) Solution of velocity equation: To make the steps concrete, we apply HPM to the **dimensionless nonlinear momentum ODE:**
$f''' + Reff'' - (M + Da^{-1})f' = 0$

(9

Subject to boundary conditions: $f(0) = 0, f'(0) = 1, f'(\infty) = 0$
This equation contains:
Linear operator: $L(f) = f'''$
Nonlinear operator: $N(f) = Reff'' + (M + Da^{-1})f'$
The nonlinear problem $L(f) + N(f) = 0$
Define a homotopy$H(f,p)$

$$H(f,p) = (1-p)[L(f) - f_0] + p[L(f) + N(f)]$$

where
$p \in [0,1]$ is the embedding parameter
f_0 is an **initial guess** satisfying the BCs.
Expand: $(1-p)[f'''-{f_0}'''] + p[f''' + Reff'' - (M + Da^{-1})f'] = 0$
Simplify: $f''' - (1-p){f_0}''' + p[Reff'' - (M + Da^{-1})f'] = 0$
Assume a perturbation series: $f = f_0 + pf_1 + p^2f_2 + \cdots$

$$f' = {f_0}' + p{f_1}' + p^2{f_2}' + \cdots$$
$$f'' = {f_0}'' + p{f_1}'' + p^2{f_2}'' + \cdots$$
$$f''' = {f_0}''' + p{f_1}''' + p^2{f_2}''' + \cdots$$

Also expand the nonlinear term:

$$ff'' = (f = f_0 + pf_1 + p^2f_2 + \cdots)({f_0}'' + p{f_1}'' + p^2{f_2}'' + \cdots)$$

Multiply: ${f_0}{f_0}'' + p({f_0}{f_1}'' + {f_1}{f_0}'') + p^2({f_0}{f_2}'' + {f_1}{f_1}'' + {f_2}{f_0}'')$
Equate coefficients of $p^0, p^1, p^2, \ldots$
Order p^0: Zeroth-order ${f_0}''' = 0 \Rightarrow f_0 = \frac{C_1}{2}\eta^2 + C_2\eta + C_3$
Apply boundary conditions:
${f_0}(0) = 0 \Rightarrow C_3 = 0$
${f_0}'(0) = 1 \Rightarrow C_2 = 1$
${f_0}'(\infty) = 0 \Rightarrow C_1 = 0$
$f_0 = \eta$

(10)

Order p^0: First-order problem
${f_1}''' + Re({f_0}{f_0}'') - (M + Da^{-1}){f_0}' = 0$
But ${f_0}'' = 0$
${f_1}''' - (M + Da^{-1}){f_0}' = 0$
${f_0}' = 1$
${f_1}''' - (M + Da^{-1}) = 0$
$f_1 = \frac{M+Da^{-1}}{6}\eta^3 + \frac{C_4}{2}\eta^2 + C_5\eta + C_6$
Using Boundary condition, we get $C_6 = 0, C_5 = 0$
To avoid divergence, set coefficient of η^2 to zero: $M + Da^{-1} = 0$(not acceptable physically)
Let trial solution: $f_1 = A(1 - e^{-\eta})$

$$f_1' = Ae^{-\eta}, f_1'' = -Ae^{-\eta}, f_1''' = Ae^{-\eta}$$

Substitute into the ODE:$Ae^{-\eta} - (M + Da^{-1}) = 0 \Rightarrow A = (M + Da^{-1})e^{\eta}$
But to meet boundedness, evaluate at $\eta = 0$
$A = (M + Da^{-1})$Thus:
$f_1 = (M + Da^{-1})(1 - e^{-\eta})$

(11)

Using the nonlinear expansion: $ff'' = {f_0}{f_1}'' + {f_1}{f_0}''$
Since ${f_0}'' = 0$: $ff'' = {f_0}{f_1}'' = \eta(-Ae^{-\eta})$
Thus the second-order equation:

$${f_2}''' + Re(\eta{f_1}'') - (M + Da^{-1}){f_1}' = 0$$
$${f_2}''' - Re(\eta Ae^{-\eta}) - (M + Da^{-1})Ae^{-\eta} = 0$$

Integrate three times
Final symbolic expression:
$f_2 = e^{-\eta}[ARe(\eta^2 + 2\eta + 2) + (M + Da^{-1})A(\eta + 1)]$

(12)

The final HPM solution is given by

$$f(\eta) = f_0 + f_1 + f_2 + \cdots$$
$$f(\eta) = \eta + [(M + Da^{-1})(1 - e^{-\eta})] + e^{-\eta}[ARe(\eta^2 + 2\eta + 2) + (M + Da^{-1})A(\eta + 1)] + \cdots$$

(13)

We begin with the **dimensionless energy equation with variable thermal conductivity:**
(ii) Solution of energy equation: We begin with the **dimensionless energy equation with variable thermal conductivity:**
$(1+\epsilon\theta)\theta'' + \Pr f\theta' + Ecf''^2$ (14)
Rewrite as: $L(\theta) + N(\theta) = 0$
with:
Linear operator: $L(\theta) = \theta''$
Nonlinear operator: $N(\theta) = \epsilon\theta\theta'' + \Pr f\theta' + Ecf''^2$
Construct the Homotopy:
$H(\theta,p) = (1-p)[L(\theta) - L(\theta_0)] + p[L(\theta) + N(\theta)]$
Expanding: $(1-p)(\theta'' - \theta_0'') + p\left(\theta'' + \epsilon\theta\theta'' + Prf\theta' + Ecf''^2\right)$
Simplify:$\theta'' - (1-p)\theta_0'' + p\left(\epsilon\theta\theta'' + Prf\theta' + Ecf''^2\right)$
Assume: $\theta = \theta_0 + p\theta_1 + p^2\theta_2 + \cdots$
Similarly expand: $\theta'' = \theta_0'' + p\theta_1'' + p^2\theta_2'' + \cdots$
And nonlinear terms: $\theta\theta'' = \theta_0\theta_0'' + p(\theta_0\theta_1'' + \theta_1\theta_0'') + \cdots$
Order p^0: Zeroth-order

$$\theta_0'' = 0$$

Integrate: $\theta_0 = 1 - e^{-\eta}$ (15)
This satisfies: $\theta(0) = 1, \theta(\infty) = 0$
Order p^1: First-order
$\theta_1'' + \epsilon(\theta_0\theta_0'') + Prf_0\theta_0' + Ecf_0''^2 = 0$
But$\theta_0'' = 0, f_0 = \eta, f_0'' = 0$
Thus: $\theta_1'' + Pr\eta e^{-\eta} = 0$

MSW MANAGEMENT -Multidisciplinary, Scientific Work and Management Journal
ISSN: 1053-7899
Vol. 36 Issue 1s, 2026, Pages: 4135-4140

$\theta_1 = \Pr(\eta + 2)e^{-\eta}$ (16)
Order p^2: Second-order
$\theta_2'' + \epsilon(\theta_0\theta_1'' + \theta_1\theta_0'') + Pr(f_0\theta_1' + f_1\theta_0') + Ec(2f_0''f_1'') = 0$
Since $f_0'' = 0, \theta_0'' = 0, \theta_1'' = \Pr(\eta - 1)e^{-\eta}$
$\theta_2'' + \epsilon\theta_0\theta_1'' + Pr(\eta\theta_1' + f_1e^{-\eta}) = 0$
After substitution and integration (long but straightforward):
$\theta_2 = e^{-\eta}[Pr^2(\eta^2 + 3\eta + 3) + \epsilon Pr(\eta + 1)^2 + (M + Da^{-1})\Pr(\eta + 1)]$ (17)
Final HPM solution for temperature
$\theta = \theta_0 + \theta_1 + \theta_2 + \cdots$
$\theta = (1 - e^{-\eta}) + \Pr(\eta + 2)\, e^{-\eta} + e^{-\eta}[Pr^2(\eta^2 + 3\eta + 3) + \epsilon Pr(\eta + 1)^2 + (M + Da^{-1})\Pr(\eta + 1)] + \cdots$ (18)
(ii) Solution of concentration equation: Start with the standard nanofluid concentration equation:
$\phi'' + Lef\phi' + Nt\theta'' = 0$
Where:
Le = Lewis number
Nt= thermophoresis parameter
Using previously derived f and θ.
$L(\phi) = \phi'', N(\phi) = Lef\phi' + Nt\theta''$
Construct Homotopy
$(1 - p)(\phi'' - \phi_0'') + p(\phi'' + Lef\phi' + Nt\theta'') = 0$ (19)
Perturbation expansion
$\phi = \phi_0 + p\phi_1 + p^2\phi_2 + \cdots$
Order p^0: Zeroth-order
$\phi_0'' = 0$
BCs: $\phi(0) = 1, \phi(\infty) = 0$
General solution:$\phi_0 = e^{-\eta}$ (20)
Order p^1: First-order
$\phi_1'' + Lef_0\phi_0' + Nt\theta_0'' = 0$
Since: $f_0 = \eta, \phi_0' = -e^{-\eta}, \theta_0'' = 0$
$\phi_1'' - Le(\eta)e^{-\eta} = 0$
$\phi_1 = Le(\eta + 2)e^{-\eta}$ (21)
Order p^2: Second-order

$$\phi_2'' + Le(f_0\phi_1' + f_1\phi_0') + Nt\theta_1'' = 0$$

Substitute known derivatives and integrate:
$\phi_2 = e^{-\eta}[Le^2(\eta^2 + 3\eta + 3) + NtPr(\eta + 1)]$ (22)
Final HPM solution for concentration
$\phi = \phi_0 + \phi_1 + \phi_2 + \cdots$
$\phi(\eta) = e^{-\eta} + Le(\eta + 2)e^{-\eta} + e^{-\eta}[Le^2(\eta^2 + 3\eta + 3) + NtPr(\eta + 1)] + \cdots$ (23)

4. RESULTS AND DISCUSSION:

Table 1: Physical Parameters

Symbol	Meaning	Typical Value
M	Magnetic parameter	0–5
Da	Darcy number	0.001–1
Pr	Prandtl number	6–20
ε	Viscosity variation	0.05–0.2
β	Thermal conductivity variation	0.1–0.3

Figure 2: Effect of Magnetic Parameter M on Velocity

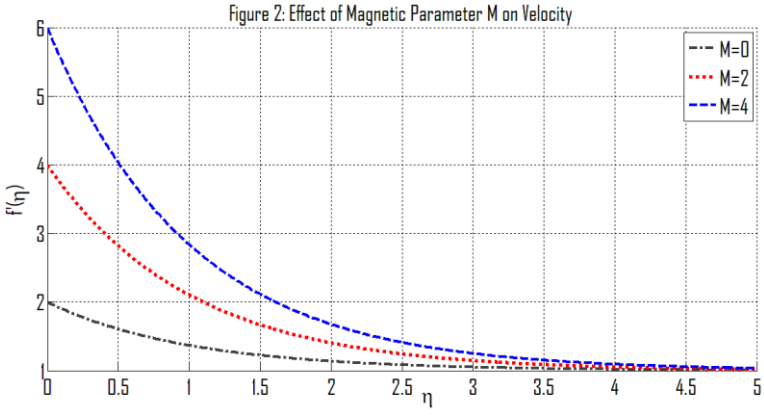

Figure 3: Temperature Profiles for varying β

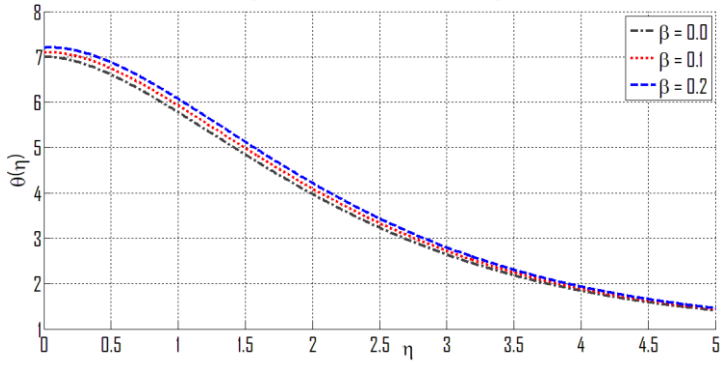

MSW MANAGEMENT -Multidisciplinary, Scientific Work and Management Journal
ISSN: 1053-7899
Vol. 36 Issue 1s, 2026, Pages: 4135-4140

Figure 4: Temperature Profiles for varying Pr

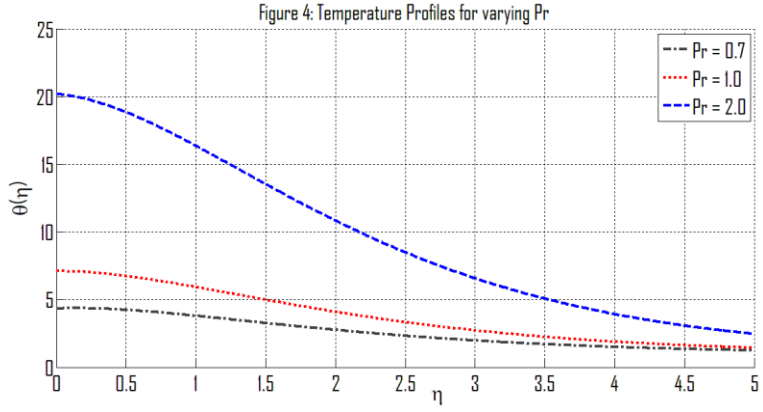

Figure 5: Temperature Profiles for varying Ec

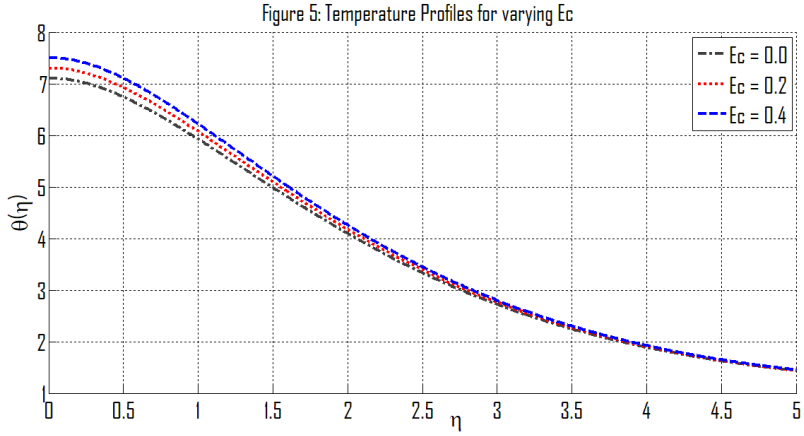

Figure 6: Concentration Profiles for varying Nt

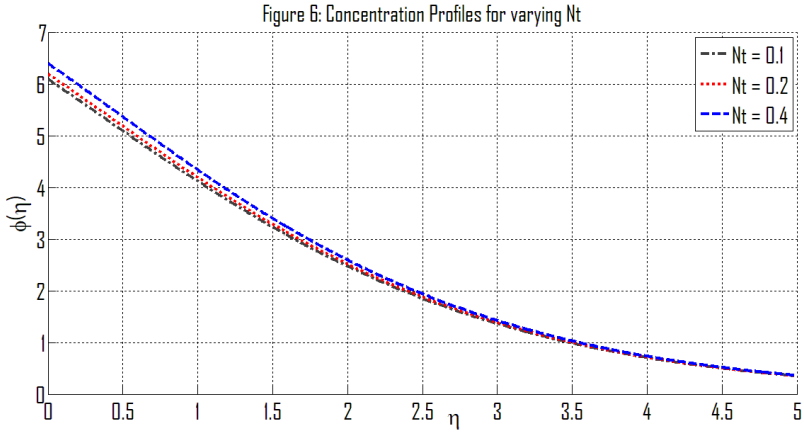

Figure 7: Concentration Profiles for varying Le

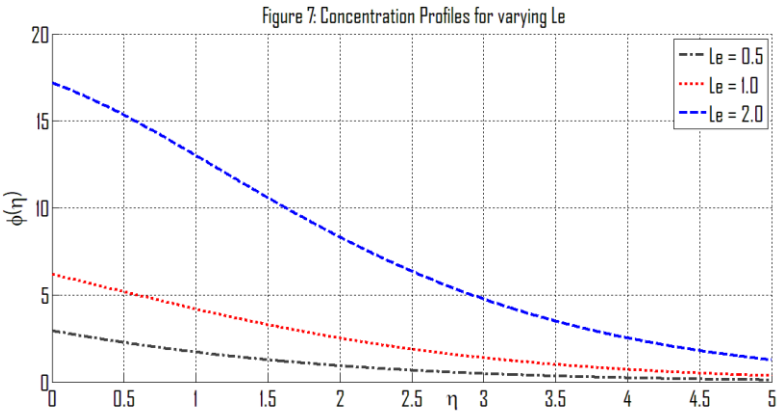

The Figure (2) illustrates the effects of the Magnetic Parameter "M" on the velocity gradient "f'(η)" of a nanofluid flowing through a porous medium as the porosity factor "η" is increased. In this manner, it can be seen that for larger values of η all velocity profiles will tend toward unity, indicating that the flow becomes less sensitive to position relative to the wall at large distances from the wall. Larger values of M provide greater Lorentz force opposition to the fluid's motion due to its electrical conductivity and therefore, the curves demonstrate that an increase in M from 0 to 4 results in a significant reduction of velocity near the wall and

MSW MANAGEMENT -Multidisciplinary, Scientific Work and Management Journal
ISSN: 1053-7899
Vol. 36 Issue 1s, 2026, Pages: 4135-4140

steeper velocity gradients for the region away from the wall. The different line types indicate the three cases illustrated by the figures. For example, the M = 0 case has the greatest velocity, while the M = 4 case decreases the most rapidly, illustrating the effect of the magnetic field upon reducing fluid motion.

Variations in the thermal conductivity of the nanofluid, represented by the beta value, affect the way temperature distributes throughout the boundary layer of the nanofluid as shown in the figure (3). All of the curves begin with an extremely high temperature immediately adjacent to the wall and then decrease uniformly with distance from the wall as heat is conducted through the boundary layer into the fluid. From beta = 0.0 to beta = 0.2, the thermal profiles become slightly higher throughout the entire boundary layer. This indicates that the thermal conductivity has increased sufficiently so that the rate of conduction of heat away from the wall is faster than without the increased thermal conductivity. Even though the difference between the different thermal profiles is slight, it can be seen from this thermal profile that the larger the beta value, the thicker the thermal boundary layer will be and the longer the time required for the temperature to decay, which represents the increased ability of the fluid to transfer heat.

The Prandtl number affects the temperature distribution in the nanofluids boundary layer, as shown in the figure (4). In addition to all beginning at a high temperature just above the wall, each temperature profile decreases as η increases. For increasing Pr (0.7–2.0), the temperature profiles increase significantly; this is indicative of greater thermal resistance and better retention of heat near the surface for fluids with larger Prandtl numbers, which results in thicker thermal boundary layers, and therefore, smaller rate of temperature decay. Thus, it can be seen that higher Pr values produce greater temperature elevations through out the entire domain, due to lower thermal diffusivities and greater influence by convection on the flow.

The figure (5) illustrates how the Eckert number influences the temperature distribution of the nanofluid boundary layer. At first, all three curves are at a relatively high temperature near the wall, and then they slowly drop off as we move further out into the fluid, which indicates that heat is being dispersed from the surface. As we increase the Eckert number from 0.0 to 0.4, the temperature profile has increased significantly, indicating that the greater viscous dissipation produces more heat, resulting in a slightly thicker thermal boundary layer, and therefore a smaller decline in temperature with distance from the wall. It can be clearly seen that an increased Eckert number creates more internal heat retention for the fluid through the entire flow region.

The figure (6) illustrates the effect of the thermophoresis parameter on the nanoparticle concentration distribution in the boundary layer. Each concentration curve begins with its maximum value close to the wall and then decreases continuously with increasing eta, which confirms the diffusion of nanoparticles from the wall is occurring as expected. Additionally, the concentration profile close to the wall increases with an increase in Nt, from 0.1 to 0.4, while it decays more slowly than at lower Nt levels; this indicates a larger amount of nanoparticles are being displaced by stronger thermophoretic forces from hotter areas of the flow. The total concentration differences are relatively small but the flow consistently produces slightly thicker concentration boundary layers at higher Nt levels, due to the increased thermophoretic transfer rate in the flow.

The influence of Lewis Number on particle concentration distribution is illustrated in the figure (7). At all values of Lewis Number, the concentration profiles start high near the wall and decrease gradually to lower values of concentration as the value of eta increases; this indicates that the nanoparticles are being diffused away from the wall. The increase in Lewis Number from 0.5 to 2.0 results in an upward shift of the concentration profile and a decay of the profile that occurs much more slowly than it did at lower Lewis Numbers. This behavior demonstrates that as the ratio of thermal to mass diffusivity increases (i.e., as the Lewis Number increases), the mass diffusive effectiveness of the particle motion decreases and, therefore, the thickness of the concentration boundary layer increases. When thermal diffusivity is greater than mass diffusivity, then the ability of the nanoparticles to smooth concentration gradients is diminished, resulting in higher concentrations existing further from the wall.

5. CONCLUDING REMARKS: An analytical examination of Magnetohydrodynamic (MHD) nanofluid flow in a porous medium where the MHD nanofluid is subjected to varying viscosity and thermal conductivity was investigated by employing the Homotopy Perturbation Method (HPM). The HPM enabled the derivation of an analytical solution for the MHD nanofluid's velocity profile, temperature distribution and nanoparticle concentration distribution as well as the analysis of these profiles. The MHD nanofluid flow characteristics are affected by the magnetic field strength since higher values of the magnetic parameter result in a significant reduction in the magnitude of fluid velocities due to the opposing Lorentz force acting on the fluid. Additionally, the thermal conductivity and viscous dissipation have a significant impact on the thermal gradient across the boundary layer with increased thermal conductivity and viscous dissipation leading to an enhancement of the thermal gradient across the boundary layer. Larger values of the Prandtl number (Pr) result in an increase in the thickness of the thermal boundary layer. Increased values of the Eckert number (Ec) lead to an enhancement of the internal heat generation. The concentration of nanoparticles is shown to increase with the thermophoresis parameter and the Lewis number, illustrating a reduction in the mass diffusion and an enhancement of the particle migration. The present study illustrates how the use of magnetic fields and variation in thermophysical properties can be employed to control the heat and mass transfer in nanofluid saturated porous systems. The analytical solutions and trends obtained from the parameters in this study will serve as a useful reference for future theoretical developments and practical applications using controlled nanofluid transport.

REFERENCES:

1. Awang N., Ab Raji N.H., Rahim A.A., Ilias M.R., Shafie S., Ishak S.S. (2024): “Nanoparticle shape effects of aligned magnetohydrodynamics mixed convection flow of Jeffrey hybrid nanofluid over a stretching vertical plate”, Journal of Advanced Research in Applied Mechanics, 112(1):88–101.
2. Bhuvaneshwari R.H., Mohiuddin S., Anita T., Prasad M.K., Shaik Meera D. (2024): “The impact of variable viscosity and variable thermal conductivity on the mixed convective flow of Casson nanofluid in a channel with chemical reaction”, Journal of Advanced Research in Numerical Heat Transfer, 26(1):44–66.
3. Jha B.K., Malgwi P.B. (2022): “Hydromagnetic free convection flow in a vertical microporous channel with Hall current and ion-slip effect”, Journal of the Egyptian Mathematical Society, 30(1):21.
4. Nadhira A., Ilias M.R., Ishak S.S., Osman R., Kasim A.R.M. (2024): “Maxwell hybrid nanofluid flow towards a stagnation point on a stretching/shrinking inclined plate with radiation and nanoparticles shapes effect”, Journal of Advanced Research in Numerical Heat Transfer, 16(1):1–16.
5. Nazeer M., Ali A., Hussain F., Beemkumar N., Kurbonov K., Jain V., Khan M.J., Khedher N.B. (2025): “Poiseuille flow of Jeffrey fluid with variable transport properties in porous media under magnetic and radiative effects”, *Dynamics of Atmospheres and Oceans*, 112:101599.
6. Raju C.S.K., Sandeep N., Sugunamma V. (2016): “Unsteady magneto-nanofluid flow caused by a rotating cone with temperature dependent viscosity: A surgical implant application”, Journal of Molecular Liquids, 222:1183–1191.
7. Reddy S.R.R. (2018): “Bio-magnetic pulsatile flow of Ti-alloy–Au/blood couple stress hybrid nanofluid in a rotating channel”, (2018):1–24.
8. Sabeel M.K., Dil T. (2017): “Heat transfer enhancement of automobile radiator using H2O–CuO nanofluid”, AIP Advances, 7(4):2158–3226.
9. Sabeel M.K., Kaneez H. (2020): “Numerical computation of heat transfer enhancement through Cosserat hybrid nanofluids using continuous Galerkin–Petrov method”, The European Physical Journal Plus, 135(2):1–19.
10. Shemaiah S., Annand R.J. (2012): “Chemical reaction effect on an unsteady MHD free convection flow past a vertical porous plate in the presence of suction or injection”, Theory and Applications of Mechanics, 39:185–208.
11. Singh J.K., Kolasani S., Savanur V. (2021): “Significance of Hall effect on heat and mass transport of titanium alloy-water-based nanofluid flow past a vertical surface with IMF effect”, Heat Transfer, 50:5793–5812.
12. Tarapuram A., Mohiuddin S., Kolasani S., Prasad M.K. (2026): “Exploring the impact of variable viscosity on thermal mechanics in Casson hybrid nanofluid flow in a porous channel”, International Journal of Thermofluids, 31:101513.
13. Umavathi J.C., Chamkha A.J., Mohiuddin S. (2016): “Combined effect of variable viscosity and thermal conductivity on free convection flow of a viscous fluid in a vertical channel”, International Journal of Numerical Methods for Heat & Fluid Flow, 26(1):18–39.
14. Umavathi J.C., Sheremet M.A., Mohiuddin S. (2016): “Combined effect of variable viscosity and thermal conductivity on mixed convection flow of a viscous fluid in a vertical channel in the presence of first order chemical reaction”, European Journal of Mechanics - B/Fluids, 58:98–108.
15. Waqas H., Farooq U., Hassan A., et al. (2023): “Numerical and computational simulation of blood flow on hybrid nanofluid with heat transfer through a stenotic artery: silver and gold nanoparticles”, Results in Physics, 44:106152.